



A design of dual guided modes ring-based photonic crystal fiber supporting 170 + 62 OAM modes with large effective mode field area

Manxing Yang¹ · Weici Liu² · Yongkang Song¹ · Jianan Wang¹ · Zhongchao Wei¹ · Hongyun Meng¹ · Hongzhan Liu¹ · Zhenming Huang¹ · Liujing Xiang¹ · Haoxian Li¹ · Faqiang Wang¹

Received: 15 July 2021 / Accepted: 13 January 2022 / Published online: 4 February 2022
© The Author(s), under exclusive licence to Springer-Verlag GmbH Germany, part of Springer Nature 2022

Abstract

In this paper, a dual guided modes ring-based photonic crystal fiber (PCF) is designed in which two channels occupying different spatial positions are independent of each other and support up to 170 + 62 orbital angular momentum (OAM) modes in the dual guided modes regions. The designed PCF consists of a large central air hole, two high refractive index rings based on Schott glass (BAK1) and cladding. The characteristics of the designed PCF are analyzed by finite element method (FEM). The results show that the proposed PCF has a sufficiently large effective refractive index difference, relatively flat dispersion, large effective mode field area and low nonlinear effects with the wavelength range from 1.45 to 1.75 μm . The energy of the light field is mainly confined to two high refractive index rings with good isolation parameters. The values of most OAM modes purity in dual guided modes regions are greater than 0.9 and the mode quality of all eigenmodes is higher than 0.93 without phase distortion over the azimuth angle. Moreover, the confinement loss of all eigenmodes are below $1.4 \times 10^{-8} \text{ dB m}^{-1}$ where the lowest value is $1.56 \times 10^{-12} \text{ dB m}^{-1}$ at $\lambda = 1.55 \mu\text{m}$ for $\text{HE}_{13,1}$ mode. The proposed PCF has a large effective mode field area, up to $316.99 \mu\text{m}^2$. The nonlinear coefficient of HE and EH modes are less than $0.55 \text{ km}^{-1} \text{ W}^{-1}$ in the outer ring and less than $1.5 \text{ km}^{-1} \text{ W}^{-1}$ in the inner ring. In conclusion, the dual guided modes ring-based photonic crystal fiber has potential applications in large capacity data transmission in optical communications.

1 Introduction

With the rapid development of communications technology in big data era, optical fiber communication system has realized frequency, amplitude, phase, polarization, and other related multiplexing technologies. However, subject to nonlinear effects, the transmission capacity of conventional single-mode fiber is limited by its gradual approach to the Shannon limit [1]. Space division multiplexing (SDM) technology can realize the multicore fiber (MCF) or multimode fiber (MMF) multichannel by utilizing the spatial freedom

of fiber, which improves the capacity requirements of the optical communication system [2]. Mode division multiplexing (MDM) is one way to achieve SDM by transmitting different information through different modes in MMF or few-mode fibers [3]. Orbital angular momentum (OAM) is a new degree of freedom except for light intensity, phase, frequency and polarization, and is composed of the even and odd modes of the same vector modes [4–6]. The OAM modes and their multiplexing methods are considered an alternative to improve the efficiency and capacity of optical communication. The use of OAM optical fiber to transmit OAM modes is one of the primary implementations of MDM technology. The vortex beam has orbital angular momentum and the phase of the light wave is helical around the singularity along the direction of propagation which can be expressed by $\exp(il\varphi)$, where φ is the azimuthal angle and l is the topological charge number. The orbital angular momentum modes of different topological charges are orthogonal to each other. Due to the orthogonality of OAM modes, the multichannel signals can be modulated to OAM modes with different topological charges, and then the channels can be distinguished by the number of topological

✉ Faqiang Wang
fqwang@scnu.edu.cn

¹ Guangzhou Key Laboratory for Special Fiber Photonic Devices, Laboratory of Nanophotonic Functional Materials and Devices, School of Information and Optoelectronic Science and Engineering, South China Normal University, Guangzhou 510006, China

² Department of Electronic Information Engineering, Guangzhou College of Technology and Business, Foshan 528138, China

charges. These properties make vortex beam widely used in the fields of optical communications [7–9], quantum technology [10, 11], optical manipulation [12, 13] and so on.

To apply OAM multiplexing technology in optical fiber communication field, it is necessary to design an optical fiber structure suitable for OAM modes transmission with good transmission characteristics. In 2012, Martin et al. [14] designed a structure of vortex fiber and proved the feasibility of OAM mode transmission in fiber by experiment. Wang et al. [15] designed and studied a basic structure of ring optical fiber to transmit OAM modes. Photonic crystal fiber (PCF) has the characteristics of high nonlinearity, endless single-mode guiding, high birefringence and low confinement loss by adjusting its optical properties through flexible design of geometric configurations and background materials [16–24]. It is possible to design the structure of PCF to support OAM modes transmission. In 2012, Yang et al. [25] proposed a ring PCF with a high nonlinear coefficient to transmit 2 OAM modes. In 2016, Zhang et al. [26] proposed a circular PCF that supports high mode quality of OAM modes. Zhou et al. [27] proposed a novel microstructure fiber with annular core for transmitting OAM modes. In 2019, Tandjè et al. [28] used the stack-and-draw approach to fabricate a ring-core PCF that supports up to four OAM mode groups. Moreover, Kabir et al. [29] designed a circular ring-based PCF doping with Schott Sulfur difluoride (SF_2) glass in the annular region, supporting 48 OAM modes with a range of 0.20–0.55 THz. In 2020, Hassan et al. [30] proposed a hollow circular PCF to support 38 OAM modes within 1000 nm bandwidth. Moreover, Kabir et al. [31] designed two novel PCFs with well Bezier polygon air holes, which are characterized by low confinement loss and flat dispersion variation.

Effective optical fiber structure design strategy can make the optical fiber support more OAM modes transmission in the optical fiber and ensure the stability of OAM modes transmission. In 2018, Zhang et al. [32] presented a circular PCF with a high refractive index germanosilicate circular ring core to support 110 OAM modes over the 110 nm bandwidth from 1.52 to 1.62 μm . In 2019, Hong et al. [33] proposed an all-silica hollow PCF that can carry 101 OAM modes and the proposed PCF is characterized by high mode quality and low crosstalk. Huang et al. [34] designed a microstructure ring fiber with a high refractive index ring to support 146 OAM modes at 1.1 μm . There are also many studies on the modes transmission in dual guided channel regions, usually one channel transmits OAM modes and the other channel transmits linear polarization (LP) modes. In 2013, Bozinovic et al. [35] designed the scroll fiber with LP modes and OAM modes transmitted in different regions. In 2018, Xu et al. [36] designed a microstructure PCF with a dual guided modes regions, supporting 30 OAM modes and 2 LP modes. In 2020, Wang et al. [37] designed a

microstructure PCF consisting of two low refractive index rings of Schott glasses, supporting 56 OAM modes and 4 LP modes. Al-Zahrani et al. [38] proposed a ring-core PCF with Schott sulfur difluoride (SF_2) glass as the ring regions material, supporting 76 OAM modes and 6 LP modes. In 2020, Wang et al. [39] designed a nested PCF with two guided modes regions supporting 30 + 50 OAM modes.

In this paper, we designed a dual guided modes ring-based PCF structure consisting of a central air hole, two high refractive index rings and cladding. The two high refractive index rings are designed to transmit more OAM modes. The two channels that occupy different spatial positions in designed PCF are independent of each other and can support many OAM modes at the same wavelengths. The dual guided modes ring-based PCF can support 170 + 62 OAM modes with the wavelength ranging from 1.45 to 1.75 μm . It has been calculated that most of the OAM modes supported by the designed fiber have high OAM purity and the mode quality of all eigenmodes is higher than 0.93 without phase distortion over the azimuth angle. The effective refractive index difference of the OAM modes is up to 2.14×10^{-3} , which can effectively reduce the degeneracy between the vector modes and ensure the stable transmission of OAM modes. One of the advantages of the designed PCF is that it has a large effective mode field area up to 316.99 μm^2 , avoiding the suppression of nonlinear effects more effectively.

2 Design of the photonic crystal fiber

OAM $_{l,m}$ modes can be synthesized by the odd-modes and even-modes vectors of $\text{HE}_{l+1,m}$ or by the odd-modes and even-modes vectors of $\text{EH}_{l-1,m}$, which can be summarized with the following formulas [17]:

$$\text{OAM}_{\pm l,m}^{\pm} = \text{HE}_{l+1,m}^{\text{even}} \pm j\text{HE}_{l+1,m}^{\text{odd}}, \quad (1)$$

$$\text{OAM}_{\pm l,m}^{\mp} = \text{EH}_{l-1,m}^{\text{even}} \pm j\text{EH}_{l-1,m}^{\text{odd}}, \quad (2)$$

where the l is the topological charge number, and m is the radial order corresponding to the radial intensity distribution of the modes. The symbol in superscript " \pm " represents the right or left circular polarization of spin angular momentum, and the symbol in subscript " $\pm l$ " represents the right or left rotation direction of OAM modes wavefront. The superscripts "even" and "odd" represent the even mode and odd mode of the corresponding eigenmode, which are distinguished by $\pi/2$ azimuthal rotation in polarization. The number of the topological charge of OAM modes is theoretically infinite, but an optical fiber can only support limited number of OAM modes due to the limitation of optical fiber structure. Therefore, an effective optical fiber structure design

strategy is needed to enable the optical fiber to transmit more OAM modes. Besides, for the design of OAM transmission fiber, it is necessary is to make the effective refractive index difference (Δn_{eff}) between the adjacent eigenmodes ($HE_{l+1,m}$, $EH_{l-1,m}$) higher than 1×10^{-4} to avoid being coupled into LP modes due to the near-degeneracy of adjacent eigenmodes [40, 41].

The proposed dual guided modes ring-based PCF structure is presented in Fig. 1. The inner and outer radius of the ring structure is labeled by r_0 , r_1 , r_2 and r_3 . Fused silica is the background material of the designed PCF, and its refractive index is 1.444. For further increase of the communication capacity of optical fiber, we consider designing two transmission regions in a limited space to transmit more OAM modes while ensuring low crosstalk. Therefore, we set two high refractive index rings as two guided modes regions. To increase the number of OAM modes, and effective refractive index separation between adjacent eigenmodes in the fiber, the designed PCF have a high contrast in refractive indices of the fiber materials. High refractive index contrast requires a large refractive index difference between the fiber core and the fiber cladding, so Schott glass is considered as the core material for the designed PCF. However, the large refractive index difference between the fiber core and the fiber cladding will cause severe spin-orbit coupling effects. Thus, Schott glass (BAK1) was used as the material of two high refractive index rings and the refractive index is 1.555 at the wavelength of 1.55 μm . In addition, to reduce the material refractive index of the cladding and ensure a high index contrast between the OAM transmission region and the cladding, the air filling fraction should be increased as much as possible. The large center air hole radius obtains enough space to accommodate a large number of OAM modes [17]. Thus, the radius of the central air hole r_0 is

chosen as 11 μm to increase the number of OAM modes, avoiding high radial order modes. However, the increasing number of air holes in each layer will increase the difficulty of the designed PCF preform arrangement. Thus, there are four layers of air holes between the two high refractive index rings and the four layers of air holes outside the outer high refractive index ring is cladding of the designed PCF. The air holes array of the designed PCF has circular symmetry. Considering the fabrication difficulties of the designed PCF, the number of air holes in each layer between the two high index rings is $N_1 = 36$, and the number of air holes in cladding is $N_2 = 60$. The air holes separate the guide-modes regions, reducing the inter-mode crosstalk between two high refractive index ring and reducing the possibility of mode energy leakage.

The thickness of the ring core affects the separation of the effective indexes [42]. The higher radial orders modes ($m > 1$) have an annular distribution in both the light intensity and the phase, and the electric distributions of the higher radial orders modes have more than one rings, while the phase distributions of the different rings are different, which will complicate the multiplex and demultiplex OAM modes [43]. Therefore, designing thin thickness of high index rings is beneficial to maintain single radial modes. However, the thin ring-core structure is easy to cause spin-orbital coupling due to imperfect circular symmetry [17]. We calculated the radial order at different thickness (d) of the high refractive index rings. As shown in Fig. 2, the designed PCF maintain "single radial" ($m = 1$) when the thickness of the rings ranging from 1.7 to 2.0 μm . The number of supported OAM modes increases when the thickness of the ring increases, but higher radial order modes ($m > 1$) appeared when the thickness of the ring is greater than 2.0 μm .

Based on the above ideas, we designed a dual guided modes regions PCF with a large center air hole and two high refractive index rings. The parameters of the designed PCF were set as $r_0 = 11 \mu\text{m}$, $r_1 = 13 \mu\text{m}$, $r_2 = 25 \mu\text{m}$, $r_3 = 27 \mu\text{m}$, $d_1 = 2.2 \mu\text{m}$, $d_2 = 2.6 \mu\text{m}$, $d_3 = 2.9 \mu\text{m}$, $d_4 = 3.3 \mu\text{m}$,

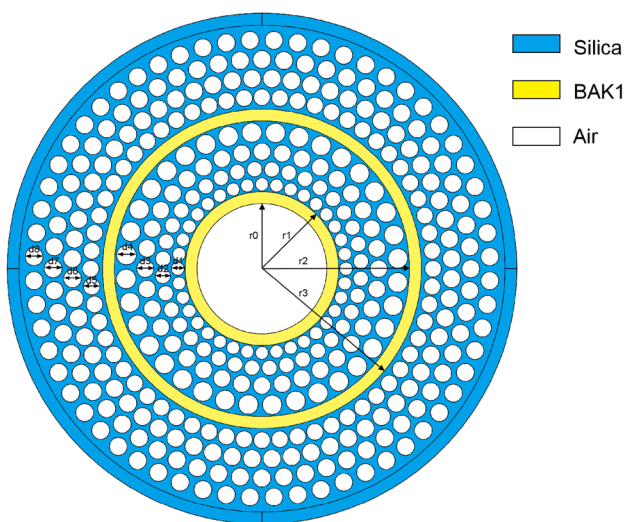


Fig. 1 Cross section of proposed dual guide modes ring-based PCF

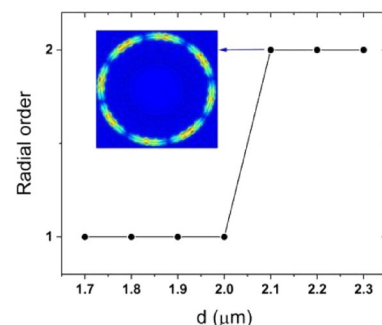


Fig. 2 The radial order at different thickness of the high refractive index rings

$d_5 = 2.9 \mu\text{m}$, $d_6 = 3.0 \mu\text{m}$, $d_7 = 3.0 \mu\text{m}$, $d_8 = 3.0 \mu\text{m}$. In this paper, the simulation software COMSOL multiphysics based on finite element method (FEM) is used, and the outermost circular perfectly matched layer (PML) of optical fiber is taken as the boundary condition. The proposed PCF supports 170 OAM modes in the outer ring and 62 OAM modes in the inner ring with 300 nm bandwidth. To distinguish OAM modes between inner ring and outer ring, the OAM modes supported by the inner ring in this paper are distinguished by label (i). We simulated the electromagnetic field intensity distributions of some eigenmodes supported in the designed fiber at $\lambda = 1.55 \mu\text{m}$, as shown in Fig. 3. It can be observed that the intensity distributions are confined in the high refractive index rings.

In addition, the normalized intensity distributions of some vector eigenmodes were calculated. Figure 4a, b show the normalized intensity distributions of the vector eigenmodes. The two annular high refractive index layers correspond to two shadow regions in Fig. 4a, b, and the peak value of normalized intensity represent the maximum of annular intensity distribution. The intensity distributions of different eigenmodes are slightly different but are mainly

confined to the ring region with a width of $2 \mu\text{m}$, indicating that all the field distributions are well confined to the high refractive index ring regions.

According to the Eqs. (1) and (2), the OAM mode is synthesized by even mode $\pm j \cdot \text{odd mode}$, so that $\text{OAM} + 8, 1 = \text{HE}_{\text{even } 9, 1} + j \cdot \text{HE}_{\text{odd } 9, 1}$, $\text{OAM} + 12, 1 = \text{HE}_{\text{even } 13, 1} + j \cdot \text{HE}_{\text{odd } 13, 1}$, $\text{OAM} + 27, 1 = \text{HE}_{\text{even } 28, 1} + j \cdot \text{HE}_{\text{odd } 28, 1}$ and $\text{OAM} + 37, 1 = \text{HE}_{\text{even } 38, 1} + j \cdot \text{HE}_{\text{odd } 38, 1}$. Therefore, we numerically calculated and obtained the intensity distributions, phase distributions and azimuthal phase variations of the above OAM modes at $\lambda = 1.55 \mu\text{m}$. In Fig. 5, the first two columns are OAM + 12, 1 and OAM + 8, 1 modes in the inner ring, and the latter two columns are OAM + 37, 1 and OAM + 27, 1 modes in the outer ring. Figure 5a–d shows that the intensity distributions of these four OAM modes are circular uniform and confined within the rings. The phase distributions of the corresponding OAM modes in the high refractive index ring have a periodic change, as shown in Fig. 5e–l. Moreover, Fig. 5i–l shows that the azimuthal phase variations of these four OAM modes have a periodic regular variation of $2l\pi$. It is

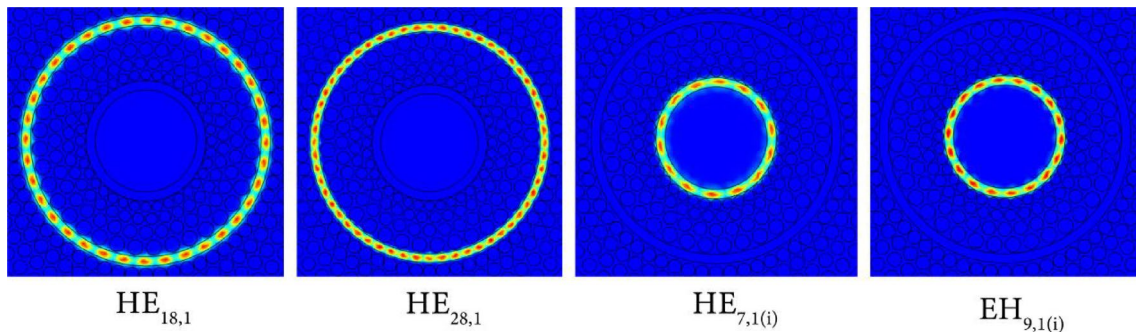


Fig. 3 The intensity distributions of $\text{HE}_{18,1}$, $\text{HE}_{28,1}$, $\text{HE}_{7,1(i)}$, and $\text{EH}_{9,1(i)}$

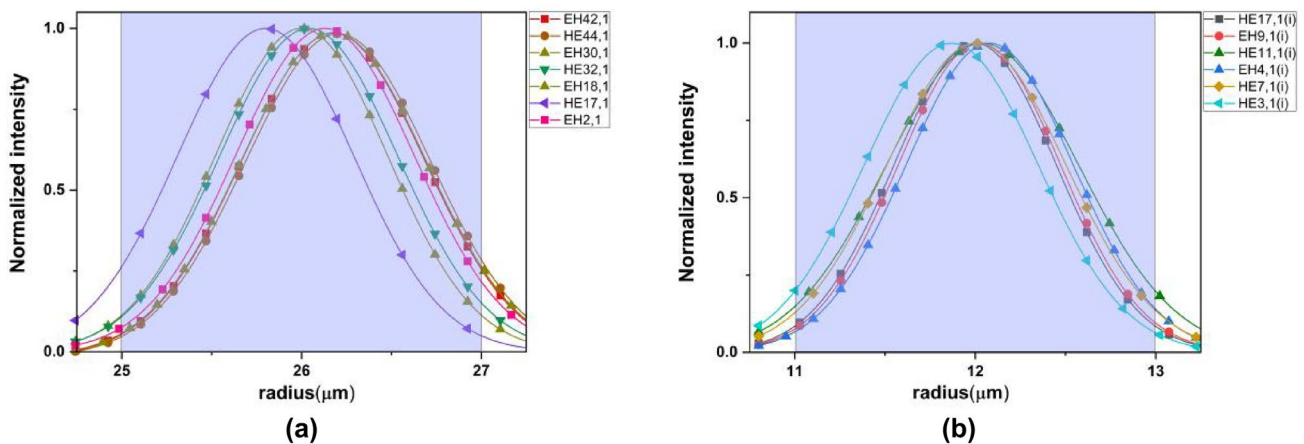


Fig. 4 **a** The normalized intensity of some eigenmodes in the outer ring. **b** The normalized intensity of some eigenmodes in the inner ring

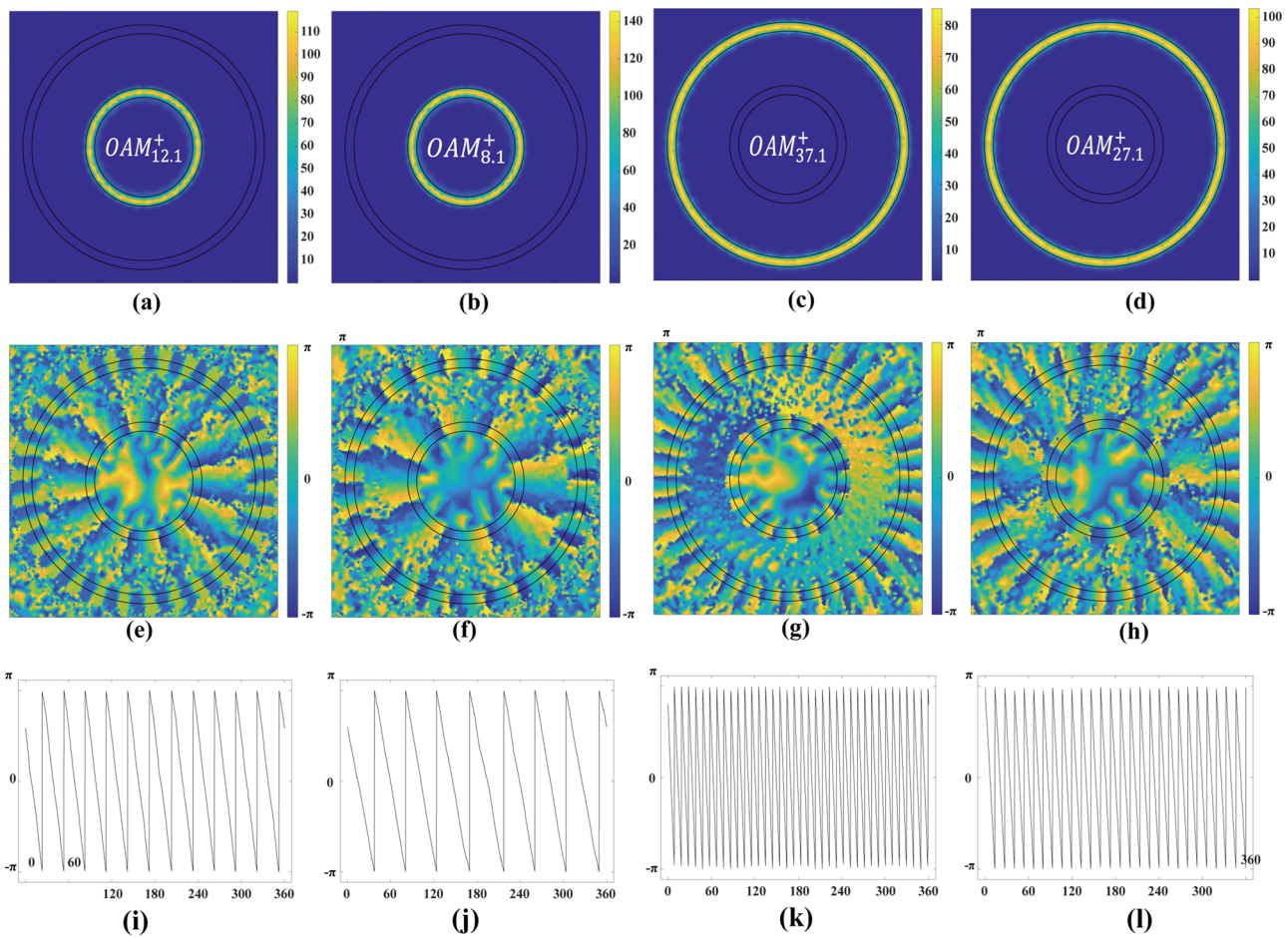


Fig. 5 The intensity distributions, phase distributions and azimuthal phase variations of **a, e, i** OAM + 12,1 and **b, f, j** OAM + 8,1 in the inner ring; the intensity distributions, phase distributions

and azimuthal phase variations of **c, g, k** OAM + 37,1 and **d, h, l** OAM + 27,1 in the outer ring

clearly seen that the azimuthal phase variations of these OAM modes are periodic regular changes without any phase distortions over the entire azimuthal angle, which means that the above OAM modes are feasible in long-distance transmission and MDM applications.

3 OAM purity

OAM purity is an important parameter for OAM mode transmission. However, due to the large refractive index contrast and relatively thin ring-core area, the OAM fiber has spin-orbit coupling effect, and there are additional modes in the fiber that are opposite to the original OAM modes [44–46]. The synthesized OAM light in fibers consists of the left-handed circularly polarized (LCP) light and the right-handed circularly polarized (RCP) light.

Higher OAM purity can effectively reduce the intrinsic crosstalk and the OAM purity can be calculated as [45]:

$$\eta = \frac{\max(\text{Power}_{\text{OAM1}}, \text{Power}_{\text{OAM2}})}{\text{Power}_{\text{OAM1}} + \text{Power}_{\text{OAM2}}} \tag{3}$$

Here, *OAM1* and *OAM2* represent two OAM light beams with opposite polarization states and topological charge difference of 2. The OAM purity (η) is defined as the power weight of the major OAM light in all the synthesized OAM lights. The purity of OAM mode is related to the spin-orbit coupling effect. The weaker the spin-orbit coupling effect, the higher the purity of OAM modes. The OAM quality of some OAM modes was numerically calculated as shown in Fig. 6. It is seen that the OAM modes purity change flat with increasing wavelength, while the values of OAM modes purity in both the outer ring and inner ring are greater than 0.9. The purity of OAM modes ensures the low intrinsic crosstalk, and the high value of

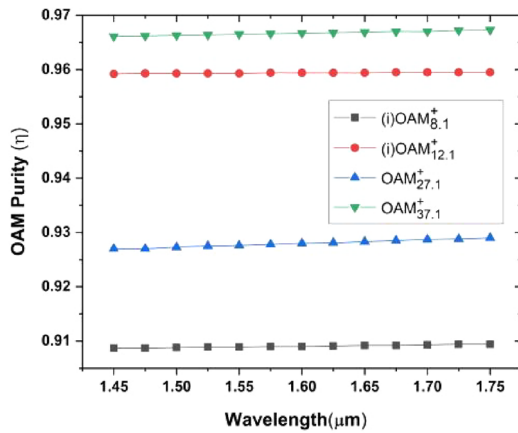


Fig. 6 OAM quality (η) of some OAM modes from 1.45 to 1.75 μm

OAM modes also guarantees the communication quality of OAM optical fiber communication.

4 Mode quality

Mode quality is an important parameter of OAM modes transmission and plays an important role in stable transmission and multiplexing of OAM modes. The OAM modes quality of the designed PCF is related to the number of OAM modes. The number of OAM modes not only relates to the capacity of transmission, but also guarantees robust transmission [47]. The mode quality of OAM modes can be calculated by the following equation [23]:

$$\eta = \frac{I_r}{I_c} = \frac{\iint_{\text{rings}} |\vec{E}|^2 dx dy}{\iint_{\text{cross-section}} |\vec{E}|^2 dx dy} \tag{4}$$

Here, I_r and I_c refer to the average intensity of the eigenmodes in the high refractive index rings and the whole section of the proposed fiber.

The mode quality of some OAM modes with increasing wavelength is calculated using the modes intensity of the ring and the total cross section of proposed PCF, and the results are shown in Fig. 7. The dual guided modes regions can be used to transmit $170 + 62$ OAM modes while more OAM modes guarantee robust transmission and high mode quality of OAM modes. The mode quality is approximately negatively correlated with increasing wavelength. Figure 7 clearly shows that the values of mode quality are all greater than 0.93 which is beneficial to the encoding and multiplexing of optical information.

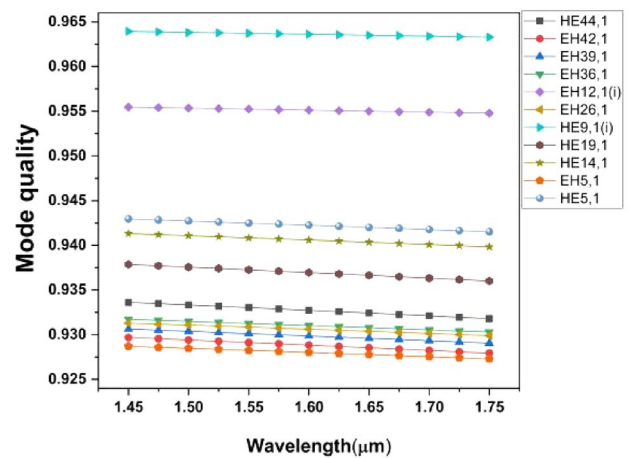


Fig. 7 Mode quality of the supporting eigenmodes from 1.45 to 1.75 μm

5 Effective refractive index and Effective refractive index difference

Figure 8a, b depicts the change in the effective refractive index of some OAM modes with the wavelength ranging from 1.45 to 1.75 μm . The effective refractive index of all eigenmodes decrease gradually with increasing wavelength. For HE or EH modes at the same wavelength, the effective refractive index of the low-order mode is higher than that of the higher-order mode. The effective refractive index differences between the eigenmodes of $\text{HE}_{l+1,m}$ and $\text{EH}_{l-1,m}$ are calculated and the results are plotted in Fig. 8c, d. At $\lambda = 1.55 \mu\text{m}$, the value of maximum Δn_{eff} of the eigenmodes supported by the outer ring is 2.13×10^{-3} , and in the inner ring, the value of maximum Δn_{eff} is 3.31×10^{-3} . Besides, the minimum Δn_{eff} of the eigenmodes supported by the outer ring and the inner ring are 0.34×10^{-3} and 0.44×10^{-3} , respectively. The designed PCF strictly keeps the effective refractive index difference of the eigenmodes above 1×10^{-4} which indicates that the corresponding eigenmodes can be well separated and ensures the stable transmission of OAM modes.

6 Dispersion properties

As the effective refractive index difference Δn_{eff} is above 10^{-4} , modal dispersion of the optical fiber is not considered. Thus, the dispersion properties of the eigenmodes constituting the OAM modes are calculated by combining the material dispersion and the waveguide dispersion, which can be expressed as [48]:

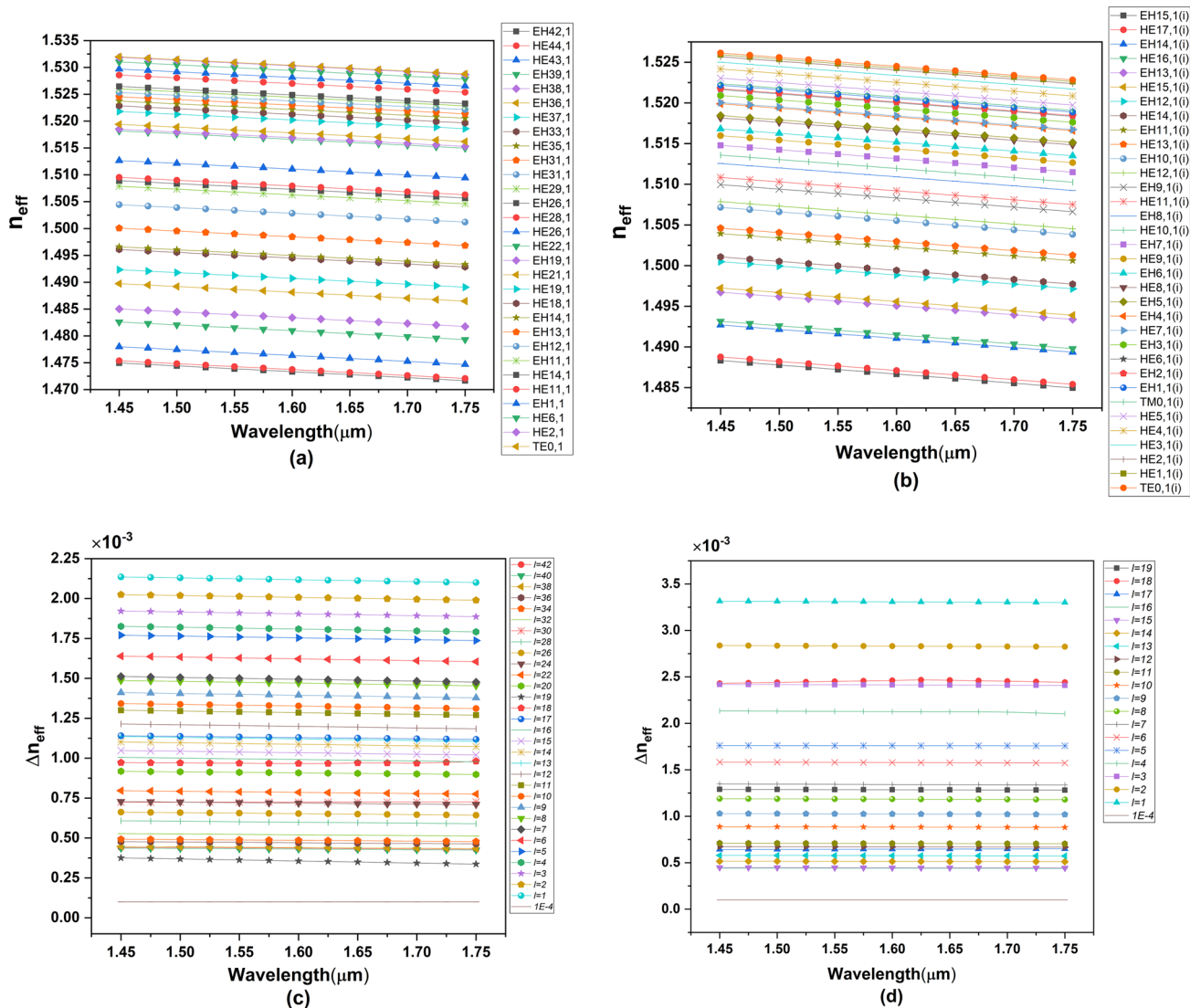


Fig. 8 The effective refractive index of eigenmodes supported by **a** outer ring and **b** inner ring. The effective refractive index difference of eigenmodes supported by **c** outer ring and **d** inner ring

$$D \approx D_w + D_m \tag{5}$$

The material dispersion D_m and the waveguide dispersion D_w are calculated, respectively, with the following formulas:

$$D_m(\lambda) = -\frac{\lambda}{c} \cdot \frac{d^2 n(\lambda)}{d\lambda^2}, \tag{6}$$

$$D_w(\lambda) = -\frac{\lambda}{c} \cdot \frac{d^2 \text{Re}\{n_{\text{eff}}\}}{d\lambda^2}, \tag{7}$$

where c is the propagation velocity of light in vacuum, λ is the wavelength of the incident light and $\text{Re}\{n_{\text{eff}}\}$ is the real part of the effective refractive index of the eigenmodes. $n(\lambda)$ is the refractive index of glass as a function of wavelength,

which can be calculated by Sellmeier dispersion equation [49]:

$$n^2 = 1 + \frac{A_1 \lambda^2}{\lambda^2 - B_1^2} + \frac{A_2 \lambda^2}{\lambda^2 - B_2^2} + \frac{A_3 \lambda^2}{\lambda^2 - B_3^2}, \tag{8}$$

where n is the refractive index of Schott glass (BAK1), λ is the wavelength of incident light, $A_1 = 1.12365662$, $A_2 = 0.309276848$, $A_3 = 0.881511957$, $B_1 = 0.00644742752$, $B_2 = 0.0222284402$, $B_3 = 107.297751$ [50].

Figure 9 show that the dispersion of the HE and EH modes supported by the outer and inner rings gradually with increasing wavelength. The dispersion changes with the increase of the topological charge number of the eigenmodes, and the dispersion increases relatively slowly

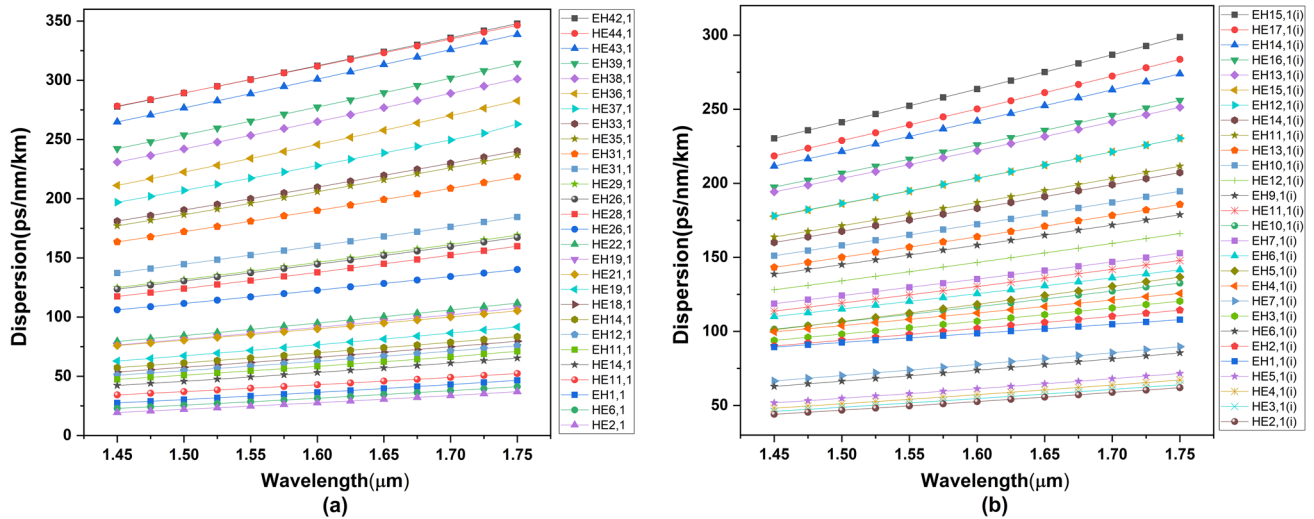


Fig. 9 a Dispersion of OAM modes supported by the outer ring. b Dispersion of OAM modes supported by the inner ring

for the lower order eigenmodes. In the range of 1.45 to 1.75 μm , the dispersion of $\text{HE}_{11,1}$ ($l=10$) has changed by $5.9 \text{ ps nm}^{-1} \text{ km}^{-1}$, that of $\text{EH}_{26,1}$ ($l=27$) has changed by $14.4 \text{ ps nm}^{-1} \text{ km}^{-1}$, and that of $\text{HE}_{35,1}$ ($l=34$) has changed by $19.6 \text{ ps nm}^{-1} \text{ km}^{-1}$, while the dispersion changes of all these modes are less than $24 \text{ ps nm}^{-1} \text{ km}^{-1}$. Therefore, the dispersion variation of the designed PCF is relatively flat.

7 Effective mode field area

The effective mode field area (A_{eff}) is related to the size of the fiber structure, such as the effective index differences and the core diameter, which can be obtained from the following formula [47]:

$$A_{\text{eff}} = \frac{\iint |E(x,y)|^2 dx dy}{\iint |E(x,y)|^4 dx dy}, \tag{9}$$

where $E(x,y)$ is the normalized electric field distribution of the generated transverse field.

Figure 10 show the effective modes field area change curve for the designed PCF with increasing wavelength. The designed dual guided modes ring-based PCF has enough large effective modes field area to improve the quality of mode transmission as large as possible. The results show that the effective modes field area of the eigenmodes is between 79.13 and $316.99 \mu\text{m}^2$ with 300 nm bandwidth. At $\lambda = 1.55 \mu\text{m}$, the maximum and the minimum effective mode field area of the modes supported by the outer ring is $315.75 \mu\text{m}^2$ ($\text{HE}_{44,1}$) and $211.70 \mu\text{m}^2$ ($\text{HE}_{1,1}$), respectively. Also, the maximum and the minimum effective mode area

of the eigenmodes supported by the inner ring is $128.58 \mu\text{m}^2$ ($\text{HE}_{16,1}$) and $79.20 \mu\text{m}^2$ ($\text{HE}_{1,1}$) respectively.

8 Nonlinear coefficient

Nonlinearity is one of the most important parameters of optical fiber. The nonlinear effects of optical fiber can limit system capacity, affect system performance, and limit relay distance, so that the small nonlinear coefficient is conducive to the transmission of OAM modes in optical fiber. The nonlinear coefficient can be calculated from the following formula [51]:

$$\gamma = \frac{2\pi n_2}{\lambda A_{\text{eff}}}, \tag{10}$$

where the nonlinear index of fused silica n_2 is $2.6 \times 10^{-20} \text{ m}^2 \text{ W}^{-1}$.

The nonlinear coefficient of the fiber is determined by the substrate material and the area of the mode field of the fiber. The effective mode field area of photonic crystal fiber is improved by increasing the central porosity, and the influence of nonlinear effect on optical fiber communication system is reduced. The wavelength and effective mode area are inversely proportional to the nonlinear coefficient. The designed PCF has a large effective modes field area and has a significant effect on suppressing nonlinear effects in the fiber. Figure 11a shows that the nonlinear coefficient decreases gradually with the increase of wavelength. All the eigenmodes of the PCF have much lower nonlinear

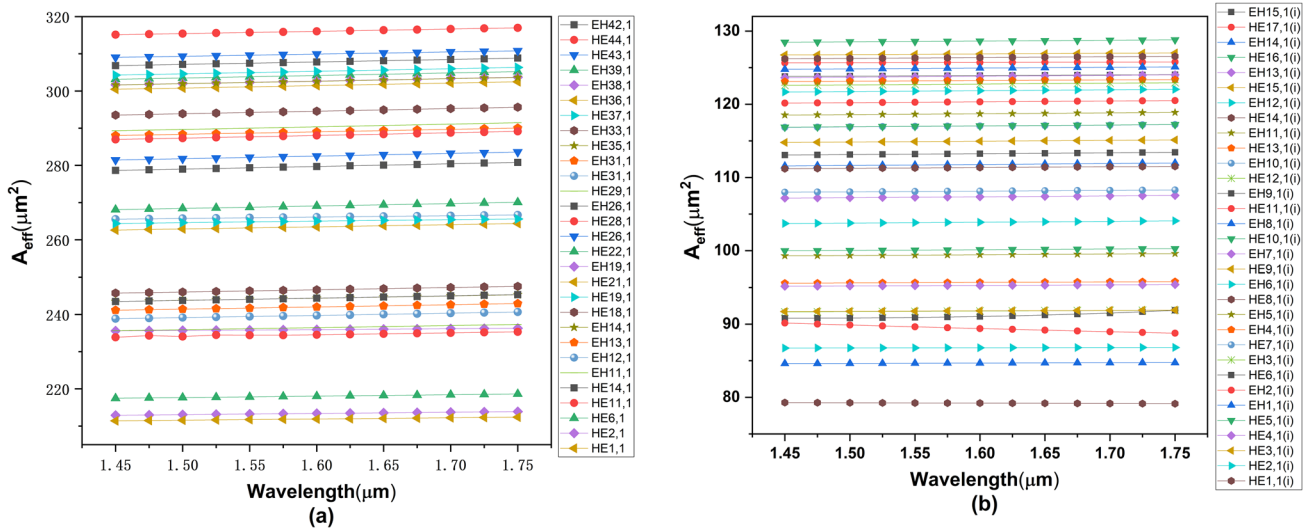


Fig. 10 **a** The effective modes field area of eigenmodes supported by the outer ring. **b** The effective modes field area of eigenmodes supported by the inner ring

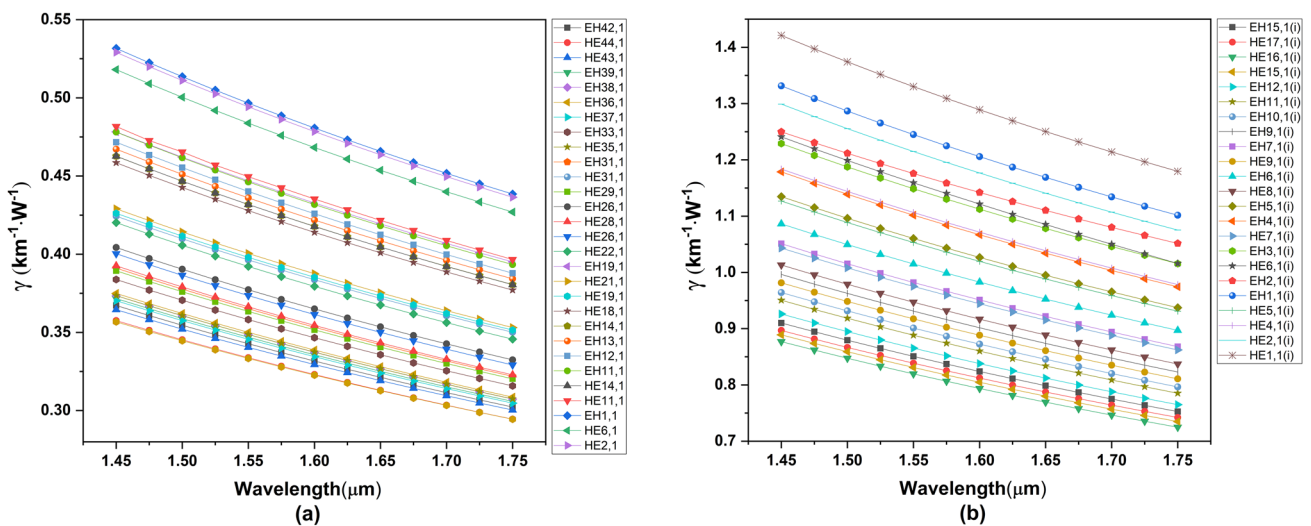


Fig. 11 **a** The nonlinear coefficient of eigenmodes supported by the outer ring. **b** The nonlinear coefficient of eigenmodes supported by the inner ring

coefficient with the wavelength range from 1.45 to 1.75 μm . The results show that the nonlinear coefficient of HE and EH modes in the outer ring is lower than $0.55 \text{ km}^{-1} \text{ W}^{-1}$, and that of all modes in the inner ring is no higher than $1.5 \text{ km}^{-1} \text{ W}^{-1}$. The lowest nonlinearity of $0.295 \text{ km}^{-1} \text{ W}^{-1}$ is obtained for $\text{HE}_{44,1}$ at $\lambda = 1.75 \mu\text{m}$. The proposed PCF with low nonlinear coefficient is beneficial to the transmission of vortex beam in optical fiber as well as the compression of nonlinear signal distortion.

9 Isolation parameters

In this paper, optical power isolation of between the communication channels in two rings high index regions is analyzed. In the designed PCF, there are four layers of air holes between the outer ring and the inner ring, which formed a large refractive index difference for isolation and reduce inter-mode crosstalk [36]. The isolation parameter (ISO) can be calculated as [52]:

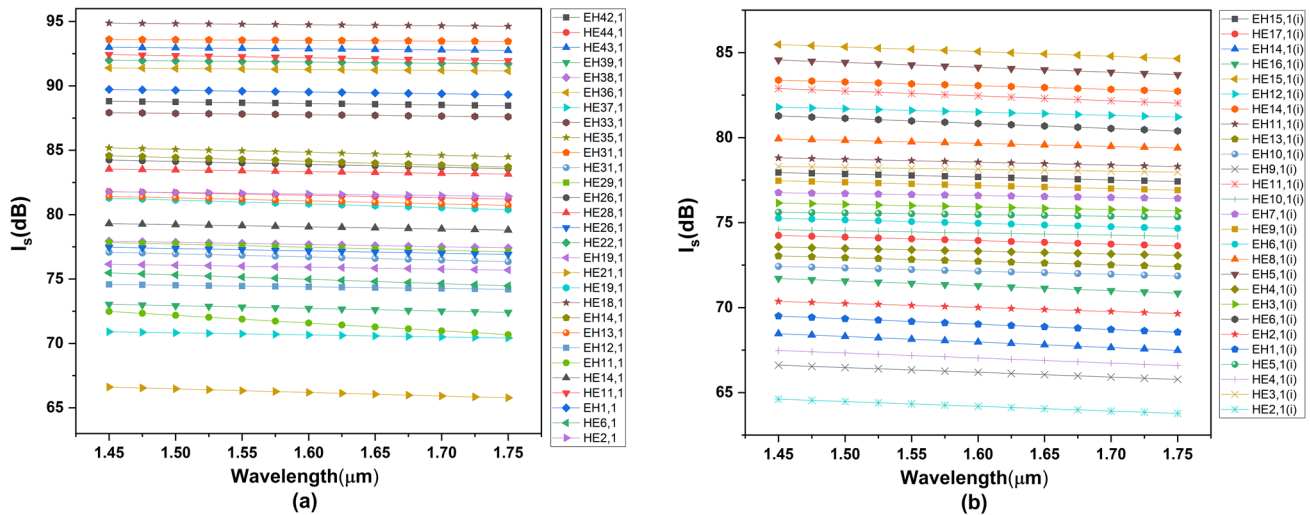


Fig. 12 **a** The isolation parameter of eigenmodes supported by the outer ring. **b** The isolation parameter of eigenmodes supported by the inner ring

$$I_{s(O \rightarrow I)} = -10 \times \log \frac{\iint_{\text{Inner}} (E_x H_y - E_y H_x) dx dy}{\iint_{\text{Total}} (E_x H_y - E_y H_x) dx dy}, \quad (11)$$

$$I_{s(I \rightarrow O)} = -10 \times \log \frac{\iint_{\text{Outer}} (E_x H_y - E_y H_x) dx dy}{\iint_{\text{Total}} (E_x H_y - E_y H_x) dx dy}. \quad (12)$$

Here, E_x , E_y and H_x , H_y are the transverse electric and magnetic fields components of the relevant modes. The isolation parameters $I_{s(O \rightarrow I)}$ and $I_{s(I \rightarrow O)}$ are introduced to measure power crosstalk from outer ring to inner ring and from inner ring to outer ring, respectively.

Figure 12a, b shows the isolation parameter varying with wavelength range from 1.45 to 1.75 μm . The high value of isolation parameter is not only beneficial to good isolation effect, but also helpful to high capacity and advantageous optical fiber communication systems. The results show that the isolation parameter is approximately negatively correlated with wavelength, and the isolation parameter in the designed PCF is above 65 dB. According to the previously published articles [36–39], the crosstalk between the channels in two rings high index regions is low and negligible. Hence, the high isolation of the designed PCF can provide a large capacity and a favorable optical fiber communications system.

10 Confinement loss

The confinement loss is an important parameter to characterize the propagation performances of the designed optical fiber, which is caused by structural defects and internal

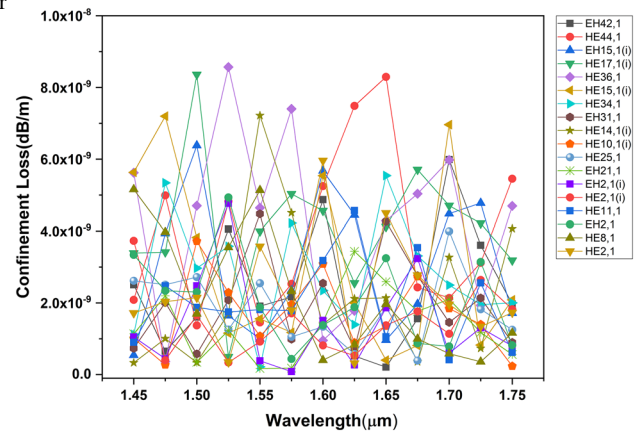


Fig. 13 The confinement loss of some eigenmodes absorption. Low confinement loss ensures the long-distance transmission of OAM modes. The confinement loss is calculated using the imaginary part of the effective index of the eigenmodes [53]:

$$C_{\text{loss}} = \frac{40\pi}{\ln(10)\lambda} \text{Im}(n_{\text{eff}}) \quad (\text{dB/m}), \quad (13)$$

where the imaginary part of the refractive index and the wavelength are labeled by $\text{Im}(n_{\text{eff}})$ and λ . The designed PCF have four layers of air hole rings and a larger air hole, which can effectively reduce the confinement loss. Figure 13 shows the values of confinement loss of some eigenmodes with increasing wavelength. At $\lambda = 1.55 \mu\text{m}$, the minimum confinement loss is $1.56 \times 10^{-12} \text{ dB m}^{-1}$ ($\text{HE}_{13,1}$). There is no linear relationship between the confinement loss and wavelength, but the confinement loss is on the order between from 10^{-12} to $10^{-8} \text{ dB m}^{-1}$ while all the values of confinement loss were lower than $1.4 \times 10^{-8} \text{ dB m}^{-1}$. The designed PCF has a lower confinement loss in the transmission of

vortex beam and it can be used for the transmission of vortex beam in the fiber communication system.

To determine the performance of the proposed PCF, we compared the proposed PCF with previously published articles. The comparison of several important parameters of PCF are shown in Table 1, which can be seen that our proposed PCF supports more OAM modes. In addition, the proposed dual guided ring-based PCF has a larger effective modes field area and a lower nonlinear coefficient.

11 Fabrication possibility

The designed PCF structure consists of a central air hole, two high refractive index rings and cladding. The designed PCF is designed to have eight layers of air holes, with an array of circular symmetry and tangent lines, which makes the fabrication of preform easier [17]. The designed PCF was made up of fused silica as the background material, and the materials of the two circular high refractive index layers are Schott glass (BAK1). The structure of the PCF is relatively complex, so we consider the feasibility to fabricate the designed PCF. First of all, the Schott glass (BAK1) is commercial glass and we can obtain them from many specialties glass companies. In 2005, Feng et al. [54] used rotary sonic drilling machine to produce porous microstructures on prefabricated bars of lead silicate glass (SF glass). Therefore, rotary sonic drilling machine is used to drill a circular hole in the center of the Schott glass, and then two high refractive index ring tubes of different radii can be obtained. In addition, six different sizes of quartz silicon glass tubes should be prepared. Then the capillary-stacking technique is used to stacked quartz silicon glass tubes along with two high refractive index ring tubes to formed preform. Finally, the temperature and drawing speed of the

fiber drawing tower are precisely controlled to prevent the collapse of air holes, and the designed dual guide modes PCF are drawn by “stack-and-draw” technology. Thus, it is also possible to fabricate the designed PCF using the above method.

12 Conclusion

In this paper, we presented a design of dual guided modes ring-based PCF which has a sufficiently large effective refractive index difference, relatively flat dispersion, large effective mode field area and low nonlinear effects with 300 nm bandwidth. The two channels occupying different spatial positions in proposed PCF are independent of each other and have good isolation parameters. The designed PCF can support up to 170 + 62 OAM modes in dual guided modes regions. The values of most OAM modes purity in dual guided modes regions are greater than 0.9 and the mode quality of all eigenmodes is higher than 0.93 without phase distortion over the azimuth angle. Furthermore, the numerical results show that the difference of effective refractive index of all the selected eigenmodes is higher than 3.4×10^{-4} and the confinement loss is lower than 1.4×10^{-8} dB m⁻¹ with 300 nm bandwidth. The nonlinear coefficient of all eigenmodes in the outer ring is lower than $0.54 \text{ km}^{-1} \text{ W}^{-1}$, while that in the inner ring is lower than $1.5 \text{ km}^{-1} \text{ W}^{-1}$. All the field distributions are well confined within the high refractive index ring without phase distortion over the azimuth angle. Therefore, the proposed PCF supports more OAM modes, larger effective mode field area and lower nonlinear effect, which is of great significance for large capacity transmission and MDM technology in modern optical communications system.

Table 1 Comparison chart with several numerical results of published articles

References	Supported mode	Effective modes field area (μm ²)	ISO (dB)	Nonlinearity (km ⁻¹ W ⁻¹)	Confinement loss (dB m ⁻¹)	Structure shape
[23]	56 OAM	< 90	–	< 4	1.7407×10^{-11}	Coil shape PCF
[24]	26 OAM	65	–	< 5	1.03×10^{-10}	Spider web-shaped PCF
[29]	48 OAM	–	267.72	–	6.91×10^{-10}	Ring-based PCF
[30]	38 OAM	72.5	–	0.997	1.534×10^{-9}	Circular PCF
[31]	42 OAM	69	–	1.0444	1.131×10^{-10}	Circular PCF
[36]	30 OAM + 2 LP	< 90	86.02	–	$\approx 10^{-10}$	Dual guided circular PCF
[37]	56 OAM + 4 LP	–	112	–	$< 4.91 \times 10^{-8}$	Circular PCF
[38]	76 OAM + 6 LP	< 9	171	–	3.72×10^{-12}	Ring-based PCF
[39]	30 + 50 OAM	92.30	> 40	1.75	–	Dual guided nested PCF
This article	170 + 62 OAM	316.99	> 65	0.295	1.56×10^{-12}	Dual guided ring-based PCF

Acknowledgements This work is supported by National Natural Science Foundation of China (Grant no. 61774062 and no. 11674109). The Science and Technology Planning Project of Guangdong Province, China (Grant no. 2017A020219007). Project of Department of Education of Guangdong Province, China (no. 2019KTSCX257).

Declarations

Conflict of interest The authors declare no conflicts of interest.

References

- R.J. Essiambre, G. Kramer, P.J. Winzer, G.J. Foschini, B. Goebel, Capacity limits of optical fiber networks. *J. Lightwave Technol.* **28**, 662–701 (2010)
- D.J. Richardson, J.M. Fini, L.E. Nelson, Space-division multiplexing in optical fibres. *Nat. Photonics* **7**, 354–362 (2013)
- P. Sillard, D. Molin, M. Bigot-Astruc, A. Amezcua-Correa, K.D. Jongh, F. Achten, 50 μm multimode fibers for mode division multiplexing. *J. Lightwave Technol.* **34**, 1672–1677 (2016)
- L. Allen, M.W. Beijersbergen, R.J.C. Spreeuw, J.P. Woerdman, Orbital angular momentum of light and the transformation of Laguerre–Gaussian laser modes. *Phys. Rev. A* **45**, 8185–8189 (1992)
- S. Ramachandran, P. Kristensen, M.F. Yan, Generation and propagation of radially polarized beams in optical fibers. *Opt. Lett.* **34**, 2525–2527 (2009)
- A.M. Yao, M.J. Padgett, Orbital angular momentum: origins, behavior and applications. *Adv. Opt. Photonics* **3**, 161–204 (2011)
- H. Huang, G. Xie, Y. Yan, N. Ahmed, Y. Ren, Y. Yue, D. Rogawski, M.J. Willner, B.I. Erkmen, K.M. Birnbaum, S.J. Dolinar, M.P.J. Lavery, M.J. Padgett, M. Tur, A.E. Willner, Tbit/s free-space data link enabled by three-dimensional multiplexing of orbital angular momentum, polarization, and wavelength. *Opt. Lett.* **39**, 197–200 (2014)
- G. Xie, Y. Ren, Y. Yan, H. Huang, N. Ahmed, L. Li, Z. Zhao, C. Bao, M. Tur, S. Ashrafi, A.E. Willner, Experimental demonstration of a 200-Gbit/s free-space optical link by multiplexing Laguerre–Gaussian beams with different radial indices. *Opt. Lett.* **41**, 3447–3450 (2016)
- Y. Yan, G. Xie, M.P.J. Lavery, H. Huang, N. Ahmed, C. Bao, Y. Ren, Y. Cao, L. Li, Z. Zhao, A.F. Molisch, M. Tur, M.J. Padgett, A.E. Willner, High-capacity millimetre-wave communications with orbital angular momentum multiplexing. *Nat. Commun.* **5**, 4876 (2014)
- M.J. Padgett, Orbital angular momentum 25 years on [Invited]. *Opt. Express* **25**, 11265–11274 (2017)
- M. Erhard, R. Fickler, M. Krenn, A. Zeilinger, Twisted photons: new quantum perspectives in high dimensions. *Light Sci. Appl.* **7**, 17146–17146 (2018)
- P. Di Trapani, W. Chinaglia, S. Minardi, A. Piskarskas, G. Valiulis, Observation of quadratic optical vortex solitons. *Phys. Rev. Lett.* **84**, 3843–3846 (2000)
- M. Padgett, R. Bowman, Tweezers with a twist. *Nat. Photon.* **5**, 343–348 (2011)
- M.P.J. Lavery, D.J. Robertson, G.C.G. Berkhout, G.D. Love, M.J. Padgett, J. Courtial, Refractive elements for the measurement of the orbital angular momentum of a single photon. *Opt. Express* **20**, 2110–2115 (2012)
- J. Wang, J.Y. Yang, I.M. Fazal, N. Ahmed, Y. Yan, H. Huang, Y. Ren, Y. Yue, S. Dolinar, M. Tur, Terabit free-space data transmission employing orbital angular momentum multiplexing. *Nat. Photonics* **6**, 488–496 (2012)
- B.K. Paul, K. Ahmed, M. Thillai Rani, K.P. Sai Pradeep, F.A. Al-Zahrani, Ultra-high negative dispersion compensating modified square shape photonic crystal fiber for optical broadband communication. *Alexandria Eng. J.* **61**, 2799–2806 (2022)
- H. Zhang, X. Zhang, H. Li, Y. Deng, L. Xi, X. Tang, W. Zhang, The orbital angular momentum modes supporting fibers based on the photonic crystal fiber structure. *Curr. Comput. Aided Drug Des.* **7**, 286 (2017)
- P.S.J. Russell, Photonic-crystal fibers. *J. Lightwave Technol.* **24**, 4729–4749 (2006)
- H. Zhang, W. Zhang, L. Xi, X. Tang, X. Zhang, A new design of a circular photonic crystal fiber supporting 42 oam modes. *Photonics and Fiber Technology 2016 (ACOFT, BGPP, NP)*, Optical Society of America, Sydney, 2016, p. Ath2C.4
- A. Nandam, W. Shin, Spiral photonic crystal fiber structure for supporting orbital angular momentum modes. *Optik* **169**, 361–367 (2018)
- M. Mehedi Hassan, K. Ahmed, B.K. Paul, M.N. Hossain, F.A. Al Zahrani, Anomalous birefringence and nonlinearity enhancement of As₂S₃ and As₂S₅ filled D-shape fiber for optical communication. *Phys. Scr.* **96**, 115501 (2021)
- N.A. Mortensen, M.D. Nielsen, J.R. Folkenberg, A. Petersson, H.R. Simonsen, Improved large-mode-area endlessly single-mode photonic crystal fibers. *Opt. Lett.* **28**, 393–395 (2003)
- M.F. Israk, M.A. Razzak, K. Ahmed, M.M. Hassan, M.A. Kabir, M.N. Hossain, B.K. Paul, V. Dhasarathan, Ring-based coil structure photonic crystal fiber for transmission of Orbital Angular Momentum with large bandwidth: outline, investigation and analysis. *Opt. Commun.* **473**, 126003 (2020)
- M.A. Kabir, M.M. Hassan, K. Ahmed, M.S.M. Rajan, A.H. Aly, M.N. Hossain, B.K. Paul, Novel spider web photonic crystal fiber for robust mode transmission applications with supporting orbital angular momentum transmission property. *Opt. Quantum Electron.* **52**, 331 (2020)
- Y. Yue, L. Zhang, Y. Yan, N. Ahmed, J.-Y. Yang, H. Huang, Y. Ren, S. Dolinar, M. Tur, A.E. Willner, Octave-spanning super-continuum generation of vortices in an As₂S₃ ring photonic crystal fiber. *Opt. Lett.* **37**, 1889–1891 (2012)
- H. Zhang, W. Zhang, L. Xi, X. Tang, X. Zhang, X. Zhang, A new type circular photonic crystal fiber for orbital angular momentum mode transmission. *IEEE Photonics Technol. Lett.* **28**, 1426–1429 (2016)
- G. Zhou, G. Zhou, C. Chen, M. Xu, C. Xia, Z. Hou, Design and analysis of a microstructure ring fiber for orbital angular momentum transmission. *IEEE Photonics J.* **8**, 1–12 (2016)
- A. Tandjè, J. Yammine, M. Dossou, G. Bouwmans, K. Baudelle, A. Vianou, E.R. Andresen, L. Bigot, Ring-core photonic crystal fiber for propagation of OAM modes. *Opt. Lett.* **44**, 1611–1614 (2019)
- M.A. Kabir, K. Ahmed, M.M. Hassan, M.M. Hossain, B.K. Paul, Design a photonic crystal fiber of guiding terahertz orbital angular momentum beams in optical communication. *Opt. Commun.* **475**, 126192 (2020)
- M.M. Hassan, M.A. Kabir, M.N. Hossain, T.K. Nguyen, B.K. Paul, K. Ahmed, V. Dhasarathan, Numerical analysis of circular core shaped photonic crystal fiber for orbital angular momentum with efficient transmission. *Appl. Phys. B* **126**, 145 (2020)
- M.A. Kabir, M.M. Hassan, M.N. Hossain, B.K. Paul, K. Ahmed, Design and performance evaluation of photonic crystal fibers of supporting orbital angular momentum states in optical transmission. *Opt. Commun.* **467**, 125731 (2020)
- L. Zhang, K. Zhang, J. Peng, J. Deng, J. Ma, Circular photonic crystal fiber supporting 110 OAM modes. *Opt. Commun.* **429**, 189–193 (2018)
- S. Hong, Y.S. Lee, H. Choi, C. Quan, Y. Li, S. Kim, K. Oh, Hollow silica photonic crystal fiber guiding 101 orbital angular

- momentum modes without phase distortion in C+L band. *J. Lightwave Technol.* **38**, 1010–1018 (2020)
34. S.-H. Huang, Q.-C. Ma, W.-C. Chen, H.-Z. Liu, X.-B. Xing, H. Cui, Z.-C. Luo, W.-C. Xu, A.-P. Luo, Microstructure ring fiber for supporting higher-order orbital angular momentum modes with flattened dispersion in broad waveband. *Appl. Phys. B* **125**, 197 (2019)
 35. N. Bozinovic, Y. Yue, Y. Ren, M. Tur, P. Kristensen, H. Huang, A.E. Willner, S. Ramachandran, Terabit-scale orbital angular momentum mode division multiplexing in fibers. *Science* **340**, 1545–1548 (2013)
 36. M. Xu, G. Zhou, C. Chen, G. Zhou, Z. Sheng, Z. Hou, C. Xia, A novel micro-structured fiber for OAM mode and LP mode simultaneous transmission. *J. Opt.* **47**, 428–436 (2018)
 37. W. Wang, N. Wang, K. Li, Z. Geng, H. Jia, A novel dual guided modes regions photonic crystal fiber with low crosstalk supporting 56 OAM modes and 4 LP modes. *Opt. Fiber Technol.* **57**, 102213 (2020)
 38. F.A. Al-Zahrani, K. Ahmed, Novel design of dual guided photonic crystal fiber for large capacity transmission in high-speed optics communications with supporting good quality OAM and LP modes. *Alex. Eng. J.* **59**, 4889–4899 (2020)
 39. W. Wang, C. Sun, N. Wang, H. Jia, A design of nested photonic crystal fiber with low nonlinear and flat dispersion supporting 30+50 OAM modes. *Opt. Commun.* **471**, 125823 (2020)
 40. C. Brunet, P. Vaity, Y. Messaddeq, S. Laroche, L.A. Rusch, Design, fabrication and validation of an OAM fiber supporting 36 states. *Opt. Express* **22**, 26117–26127 (2014)
 41. S. Ramachandran, P. Kristensen, Optical vortices in fiber. *Nanophotonics* **2**, 455–474 (2013)
 42. H. Zhang, X. Zhang, H. Li, Y. Deng, X. Zhang, L. Xi, X. Tang, W. Zhang, A design strategy of the circular photonic crystal fiber supporting good quality orbital angular momentum mode transmission. *Opt. Commun.* **397**, 59–66 (2017)
 43. S. Li, J. Wang, Multi-orbital-angular-momentum multi-ring fiber for high-density space-division multiplexing. *IEEE Photonics J.* **5**, 7101007–7101007 (2013)
 44. S. Golowich, Asymptotic theory of strong spin-orbit coupling in optical fiber. *Opt. Lett.* **39**, 92–95 (2014)
 45. Z. Zhang, J. Gan, X. Heng, Y. Wu, Q. Li, Q. Qian, D. Chen, Z. Yang, Optical fiber design with orbital angular momentum light purity higher than 99.9%. *Opt. Express* **23**, 29331–29341 (2015)
 46. Y. Yan, Y. Yue, H. Huang, J.-Y. Yang, M.R. Chitgarha, N. Ahmed, M. Tur, S.J. Dolinar, A.E. Willner, Efficient generation and multiplexing of optical orbital angular momentum modes in a ring fiber by using multiple coherent inputs. *Opt. Lett.* **37**, 3645–3647 (2012)
 47. M.M. Hassan, M.A. Kabir, M.N. Hossain, B. Biswas, B.K. Paul, K. Ahmed, Photonic crystal fiber for robust orbital angular momentum transmission: design and investigation. *Opt. Quantum Electron.* **52**, 8 (2019)
 48. Z.A. Hu, Y.Q. Huang, A.P. Luo, H. Cui, Z.C. Luo, W.C. Xu, Photonic crystal fiber for supporting 26 orbital angular momentum modes. *Opt. Express* **24**, 17285–17291 (2016)
 49. G.P. Agrawal, Nonlinear fiber optics, in *Nonlinear Science at the Dawn of the 21st Century*. ed. by P.L. Christiansen, M.P. Sørensen, A.C. Scott (Springer, Berlin, 2000), pp. 195–211
 50. Refractive Index Database, Refractiveindex.info, <https://refractiveindex.info/?shelf=glass&book=BAK1&page=SCHOTT>
 51. B.K. Paul, F. Ahmed, M.G. Mochtader, K. Ahmed, D. Vigneeswaran, Silicon nano crystal filled photonic crystal fiber for high nonlinearity. *Opt. Mater.* **84**, 545–549 (2018)
 52. M. Zhu, W. Zhang, L. Xi, X. Tang, X. Zhang, A new designed dual-guided ring-core fiber for OAM mode transmission. *Opt. Fiber Technol.* **25**, 58–63 (2015)
 53. X. Xu, H. Jia, Y. Lei, C. Jia, G. Liu, J. Chai, Y. Peng, J. Xie, Theoretical proposal of a low-loss wide-bandwidth silicon photonic crystal fiber for supporting 30 orbital angular momentum modes. *PLoS ONE* **12**, e0189660 (2017)
 54. X. Feng, A.K. Mairaj, D.W. Hewak, T.M. Monro, Nonsilica glasses for holey fibers. *J. Lightwave Technol.* **23**, 2046 (2005)

Publisher's Note Springer Nature remains neutral with regard to jurisdictional claims in published maps and institutional affiliations.